Vietnam Journal of Science and Technology ***57*** *(6) (2019) 703-713*

doi:10.15625/2525-2518/57/6/13955

SYNTHESIS OF MoS_2/GRAPHENE NANOCOMPOSITE BY FACILE ULTRASONIC-ASSISTED HYDROTHERMALMETHOD

Le Ngoc Long, Pham Trung Kien, Tran Van Khai*

Faculty of Materials Technology, Ho Chi Minh City University of Technology, VNU-HCMC
268 Ly Thuong Kiet Street, Ward 14, District 10, Ho Chi Minh City

*Email: *tvkhai1509@hcmut.edu.vn*

Received: 15 July 2019; Accepted for publication: 6 September 2019

Abstract. In this report, thin layers of MoS_2 were *in-situ* incorporated into graphene oxide (GO) to form MoS_2/graphene nanocomposite by a facile ultrasonic-assisted hydrothermal method. X-ray Diffraction (XRD) and Raman analysis revealed that the as-synthesized MoS_2 nanosheets crystalized in hexagonal phase 2H-MoS_2 while High Resolution Transmission Electron Microscopy (HRTEM) images confirmed that MoS_2 layers with average thickness of ~5–6 nm (6–8 layers) attached on the edges and surfaces of graphene sheets with high density and uniform shape restacking in three-dimensional (3D) architectures. The Scanning Transmission Electron Microscopy – Energy Dispersive X-ray spectrum (STEM-EDX) investigation further confirmed the low impurity of MoS_2/graphene composite, and the well repairing of defects in GO surfaces during the hydrothermal process. Our approach is promising for a scalable, inexpensive, and accurate strategy to fabricate state-of-the-art materials with a certain structure for various practical applications such as electrode material for Lithium battery or supercapacitor.

Keywords: MoS_2/graphene, 2D materials, graphene, hydrothermal method.

Classification numbers: 2.1.3, 2.2.2, 2.4.4.

1. INTRODUCTION

Two-dimensional (2D) materials have recently gained extensive attention for their unique structures and intriguing properties with potential applications [1, 2]. Graphene, a 2D atomic layer of sp^2 bonded carbon atoms in a hexagonal lattice [3], is one of the most studied flat materials. With fascinating properties such as high electron mobility (~200,000 $cm^2\ V^{-1}\ s^{-1}$) [4, 5], large specific surface area (~2,600 $m^2\ g^{-1}$) and excellent thermal conductivity (~5,000 $W^{-1}\ K^{-1}$) [6], graphene makes its own a promising platform for various applications. Beyond graphene, molybdenum disulphide (MoS_2) is emerging as one of the most attractive 2D materials among transition metal dichalcogenides (TMDs) group [7, 8]. With lamellar structure similar to that of graphene, a mono layer of MoS_2 compacted with Mo and S atoms forming 2D S–Mo–S covalently bonded tri-layers which in turn, stacked together by weak Van der Waals interactions along the *c*-axis to form bulk MoS_2 crystal [9]. Recently, the combination of MoS_2 and graphene to fabricate MoS_2/graphene composite has attracted significant interest. These hybrid nanostructures have exhibited better performance in comparison to their single counterparts for various applications including photocatalysts [10], batteries [11], sensing [12], and energy-harvesting [13]. Such improved performance is primarily attributed to the robust hybrid structure and the synergetic effects between few-layer MoS_2 and graphene sheets [10].

Table 1. Hydrothermal synthesis of MoS_2/graphene composite.

Synthesis method	**Precursors**	**Experiment parameters**	**Structure and morphology of composite**	**Ref.**
Hydrothermal	GO, Na_2MoO_4, and $CS(NH_2)_2$	180 °C, 24 h	MoS_2 flower-like morphology, over 12 layers	[19]
Hydrothermal and annealing	GO, trimethylamine, Na_2MoO_4 and H_2CNSNH_2	200 °C, 24 h, the product was annealed at 800 °C for 2 h in H_2 (10 %) and balanced by Ar.	MoS_2/graphene aerogel, 5–15 layers	[20]
Hydrothermal	GO, thioacetamide, ammonium heptamolybdate tetrahydrate, Citric acid	180 °C, 24 h	> 20 layers, thickness of MoS_2 sheets ~3 nm	[21]
Hydrothermal	GO, thioacetamide, ammonium heptamolybdate tetrahydrate	200 °C, 24 h	MoS_2 ~13–20 layers, lateral size of ~several micrometers	[22]
Hydrothermal and carbonization	PANI, MoO_3 and potassium thiocyanate (KSCN)	210 °C, 24 h, annealed in N_2 atmosphere at 500 °C for 4 h	MoS_2 nanoflowers ~4–12 layers, diameter ~300−700 nm, thickness ~12 nm.	[23]
Hydrothermal	3D Graphene alcogel, $Na_2MoO_4.2H_2O$ and $CS(NH_2)_2$	200 °C, 24 h	Flocculent MoS_2 nanostructures, diameter ~ 300 nm, over 20 layers	[24]
Hydrothermal	GO, $Na_2MoO_4.2H_2O$, and $CS(NH_2)_2$	240 °C, 24 h	MoS_2 ~4–5 layers	[25]
Hydrothermal	GO, $(NH_4)_2MoS_4$, DMF and $N_2H_4.H_2O$	200 °C, 12 h	Lateral size of the MoS_2 nanosheets ~50–70 nm, 12–16 layers	[26]
Hydrothermal	GO, L-cysteine and $Na_2MoO_4.2H_2O$, CTAB	240 °C, 24 h	MoS_2 with 4–6 layers and *d* (002) of 0.64 nm	[27]
Ultrasound-assisted hydrothemal	GO, thioacetamide, ammonium heptamolybdate tetrahydrate	230 °C, ~**2** h Pre-treatment the precursor of GO and MoO_4^{2-} by ultra-sonication, follow by adding reducing agent (S^{2-}) under hydrothermal condition.	MoS_2 nanopetal-like shape *in situ* grow on graphene surfaces and edges, thickness of MoS_2 petals ~5–8 nm, 6–8 layers.	This work

There are several synthesis routes of the MoS_2/graphene composites that include *ex-situ* and *in-situ* synthetic strategies. In the *ex-situ* synthetic strategy, each component materials (MoS_2, graphene or GO) are prepared separately in advance, then the composites are fabricated by layer-by-layer assembly [14], liquid phase exfoliation [15] or chemical exfoliation [16] methods. On the other hand, the *in-situ* the synthesis process involves ionic reactions such as sol-gel [17], solvothermal [18] or hydrothermal [19] methods that hold capability of synthesis nanoscale materials with uniform dispersion and complex architectures. Although hydrothermal strategies are widely used for the preparation of MoS_2/graphene materials, the reported methods often require long reaction time from several hours to several days [19–27] as shown in Table 1. Therefore, there is still a huge challenge to develop fast simple, reliable and economical synthetic routes for preparing MoS_2/graphene composites.

Here, we report facile ultrafast hydrothermal synthesis strategy on *in-situ* growth of MoS_2 nanostructure directly on GO to form MoS_2/graphene composite. Our approach is promising for a scalable, inexpensive, and accurate strategy to grow a 2D-3D MoS_2/graphene nanocomposite with different structures for potential applications in electronic and optoelectronic devices.

2. MATERIALS AND METHODS

MoS_2/graphene nanocomposite was synthesized by a facile hydrothermal method, which is a two-steps process: firstly, GO nanosheets preparation by Hummer's modified method which has been published elsewhere [28, 29] and then growing MoS_2 nanostructures on GO using a high pressure Teflon-lined stainless steel autoclave reactor (Parr Instrument Co.). All majority chemicals used in this report were purchased from Sigma Aldrich including graphite flakes (~5 µm, 99.8 %), ammonium molybdate tetrahydrate $(NH_4)_6Mo_7O_{24}.4H_2O$, 98.0 %), thioacetamide (CH_3CSNH_2, 98 %), H_2SO_4 (98 %), H_3PO_4 (85 %), $KMnO_4$ (98 %), H_2O_2 (30 wt. %).

2.1. Preparation of GO

In order to prepare a homogenous colloidal suspension of GO in deionized (DI) water, the high concentration obtained GO (~3.5 wt. %) was diluted several times with DI water (resulting concentration of 1.0 g L^{-1}), and then the mild sonication was applied for 4 h to get stable GO dispersion for the synthesis of MoS_2/graphene nanocomposite.

2.2. Synthesis of MoS_2/graphene nanocomposite

A volume ~30.0 mL of the above GO dispersion was ultrasonicated for 4 h. Then, 0.1506 g ammonium molybdate tetrahydrate was added to this solution and continued to be ultrasonicated for 2 h. Next, 0.3060 g of thioacetamide was dissolved in ~ 10 mL DI water an added to the above mixture to form a homogeneous solution (pH ~ 8–9). Subsequently, the resulting solution was transferred to a high pressure Teflon-lined stainless steel autoclave reactor (~75% volume filled), sealed, heated to 230 °C and kept at this temperature for 2 h under stirring condition. Afterwards, the reaction system was rapidly cool down to room temperature by uninstalling the autoclave out of the electric furnace. The resulting precipitate was washed several times with DI water and ethanol, then centrifuged and dried at 65 °C for 12 h in a furnace. The final MoS_2/graphene nanocomposite black powder was collected for characterization.

2.3. Characterization

X-ray diffraction (XRD) patterns were recorded using a Bruker D8 Venture diffractometer utilizing Cu Kα radiation (λ = 1.5418 Å). The morphology of the samples was observed by Field Emission Scanning electron microscopy (FESEM) (S-4800, Hitachi) and HRTEM (JEOL JEM-

2100F). The High Angle Annular Dark Field Scanning Transmission Electron Microscopy (HAADF-STEM) images were obtained with a JEM-ARM200F microscope (JEOL). Energy Dispersive X-ray (EDX) spectrum and elements mapping were obtained using an EDX spectrometer (EDX, Oxford Inca X-max 80) by STEM mode. X-ray Photoelectron Spectroscopy (XPS) analysis was performed using a monochromatized Al Kα X-ray source ($h\nu$ = 1486.6 eV) (AXIS Nova spectrometer, Kratos, UK). Micro Raman measurements were carried out using Horiba XploRA One spectrometer equipped with an Olympus BX50 microscope attachment to focus the laser beam. Green argon laser (λ = 532 nm) were used as an excitation source with liquid nitrogen-cooled CCD.

3. RESULTS AND DISCUSSION

The crystalline structure and phase components of the as-synthesized MoS_2/graphene nanocomposite were examined by XRD. As shown in Figure 1(a), the XRD pattern of GO shows a strong (001) peak at $2\theta \sim 10.8^o$ and lower (002) peak at ~23.5º, which comparing to standard diffraction pattern of GO (JCPDS 00-065-1528) confirms the GO component. For MoS_2/graphene nanocomposite, with reaction time of ~ 2 h, the XRD pattern of the MoS_2/graphene sample shows diffraction peaks at $2\theta \sim 14.4^o$, 32.5º, 39.6º and 58.9º corresponding to (002), (100), (103) and (110) crystal planes of MoS_2, respectively, which is in good agreement with 2H-MoS_2 (JCPDS 00-037-1492) [30,31] without other peaks of impurities phases. The strong (002) peak at ~14.4º corresponds to the d-spacing of ~0.63 nm, indicating that layered MoS_2 grows well along the c-axis during the synthetic process.

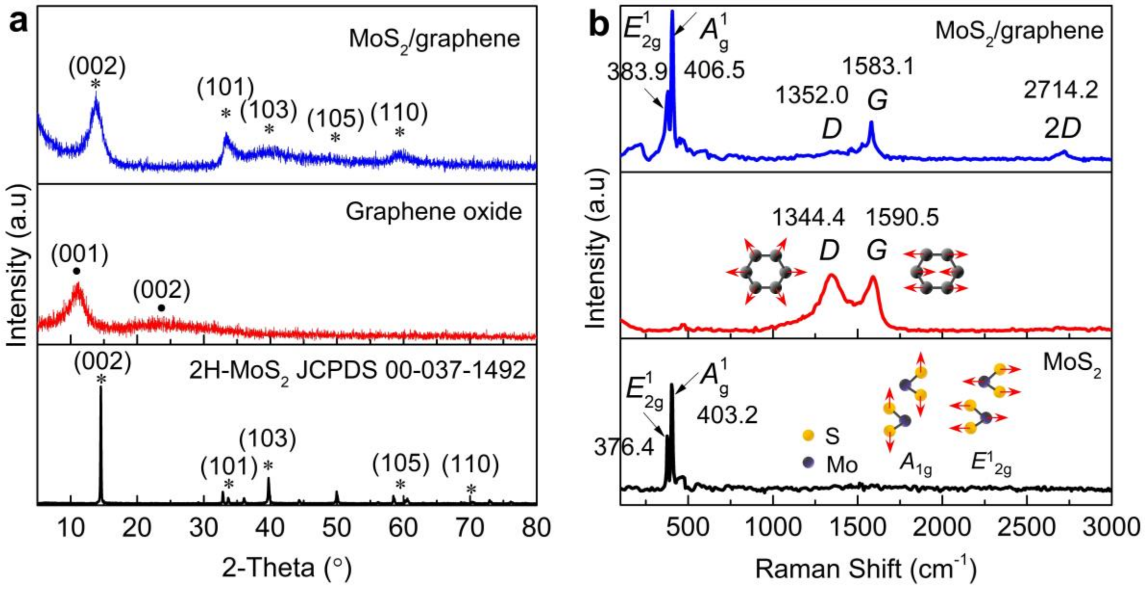

Figure 1. XRD patterns (a) and Raman spectra (b) of GO, pristine MoS_2 and MoS_2/graphene nanocomposite.

The formation of MoS_2 crystalline phase in graphene matrix can be well explained by the reduction of MoO_4^{2-} to form MoS_2 with mechanism (1) and (2) meanwhile the GO is also *in situ* reduced to graphene by H_2S during the hydrothermal process. In this case, graphene provides a platform for the nucleation and growth of MoS_2 nanostructures.

$$CH_3CSNH_2(s) + 2H_2O \rightarrow CH_3COOH + NH_3\,(g) + H_2S\,(g) \qquad (1)$$

$$4MoO_4^{2-} + 9H_2S + 6CH_3COOH \rightarrow 4MoS_2 + SO_4^{2-} + 6CH_3COO^{-} + 12H_2O \qquad (2)$$

However, the broad and low intensity of diffraction peaks compared to that of pure MoS_2 sample indicating that the MoS_2/graphene sample is in a short-range order crystalline state. It should be noted that, the Van der Waals interaction might lead to an irreversibly restacking tendency of these MoS_2 thin sheets during the growth process. This phenomenon can be explained when considering the phase transformation and structural refinement of MoS_2 when increasing reaction time [32]. The restacked structure would lead to a dramatic decrease of specific surface area of MoS_2, which is unfavorable for wide applications. The longer the reaction time, the thicker the nanopetal-like MoS_2 will be. For this reason, the total time of reaction should be less than 2 hours to get the desired crystalline structure of MoS_2/graphene nanocomposite.

Raman spectra shown in Figure 1(b) are used to analyze the structures of MoS_2/graphene nanocomposite. For MoS_2/graphene sample, two distinct peaks at ~383.9 and ~406.5 cm^{-1} represent for the *in-plane* E^1_{2g} and *out-of-plane* A^1_g vibrational modes of $2H$-MoS_2 which can be clearly identified in both spectra of MoS_2/graphene nanocomposite and pristine MoS_2 as reported elsewhere [33]. The MoS_2/graphene nanocomposite exhibit two dominant Raman peaks at ~1352 and ~1583 cm^{-1}, which match well with the D and G bands of graphene, respectively, and well agreed with that of GO [34,35]. The I_D/I_G calculated value for the MoS_2/graphene sample (I_D/I_G = ~1.06) is smaller than that of GO ($I_D/I_G = 1.60$) [34], indicating that the sp^2 conjugation is restored during the hybridization process. The decreased frequency difference of the MoS_2/graphene sample compared to pristine MoS_2 confirms the ultrathin with few layers of MoS_2 phase and matched well with HRTEM images observed in Figure 2(c, d).

The surface morphology and microstructure of MoS_2/graphene nanocomposite were examined by using FESEM and TEM as shown Figure 2(a, b). The obtained MoS_2/graphene sample has a thin sheet-like morphology joined together forming an aggregated petal-like structure. TEM image shows overall morphologies of MoS_2/graphene composite, where petal-like MoS_2 nanosheets can be clearly observed, which are well distributed on surfaces and edges of graphene sheets. It is obvious that the lateral size of the individual of graphene sheets is quite large and up to several micrometers, while MoS_2 petal-like nanosheets have diameters in range of ~200–300 nm and average thickness ~5–6 nm (6–8 layers).

To better elucidate the crystalline structure and morphological distinction between MoS_2 nanopetals and graphene, HRTEM analysis was carried out as recorded in Figure 2(c, d). As observation in Figure 2(d), MoS_2 layers grow directly on the graphene surfaces. MoS_2 occupied space with lamellar structure that can be easily distinguished from the surrounding area where hexagonal lattice of carbon in graphene clearly observed. From the HRTEM image in Figure 2(d), the spacing of ~0.63 nm can be easily measured and assigned to the distance between (002) planes of $2H$-MoS_2. Figure 2(e, f) show a schematic view of MoS_2/graphene model structures. These observations help confirming the directly growth of MoS_2 nanostructures on graphene surfaces.

To confirm the existence of graphene and MoS_2 in MoS_2/graphene composite, the HAADF-STEM and EDX spectroscopy mapping analysis were employed with the results are shown in Figure 3. The selected EDX mapping region is observed in Figure 3(a) with the elemental mapping of C, Mo, and S, respectively, in Figure 3(b–d) indicating the co-existence of C, Mo and S.

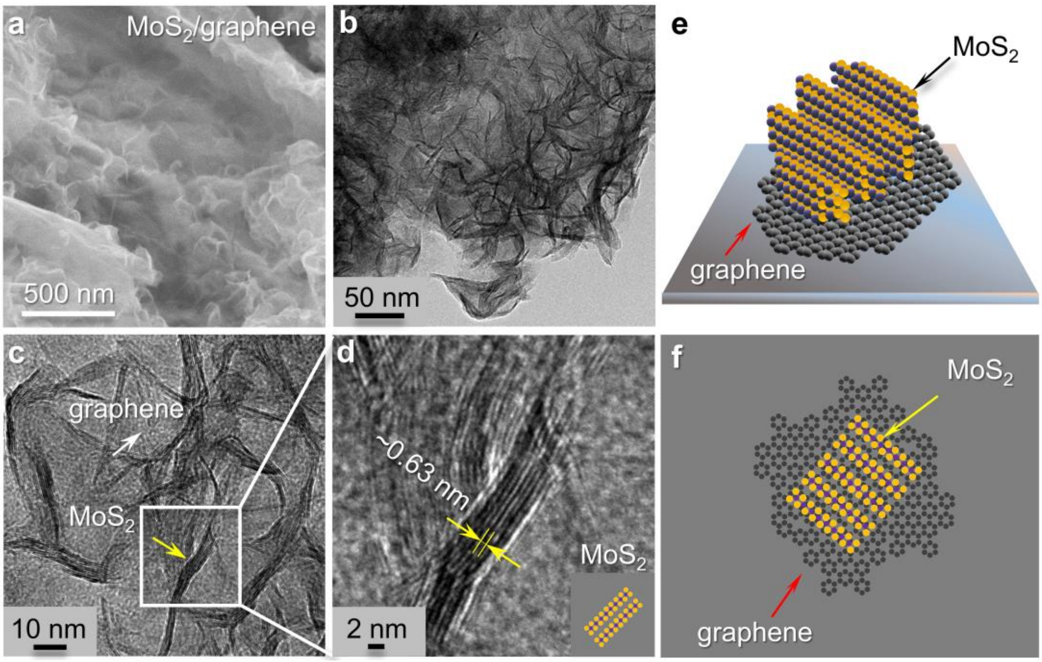

Figure 2. (a) FESEM, (b) TEM, (c, d) HRTEM images of typical morphology of MoS_2/graphene nanocomposite, (e, f) schematic view of MoS_2/graphene model structures.

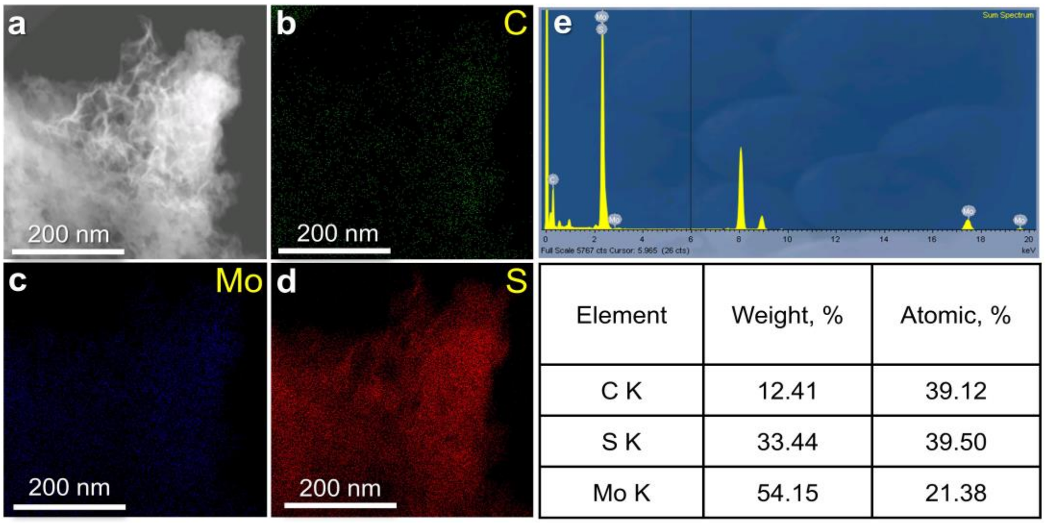

Element	Weight, %	Atomic, %
C K	12.41	39.12
S K	33.44	39.50
Mo K	54.15	21.38

Figure 3. (a) The HAADF-STEM image and the corresponding EDX elemental mapping images of (b) C, (c) Mo and (d) S for MoS_2/graphene sample; e) EDX spectrum of MoS_2/graphene.

These suggest that MoS_2 nanosheets are well attached on graphene with no serious aggregation. The chemical composition of the MoS_2/graphene sample is investigated by STEM-

EDX spectrum as recorded in Figure 3(e). The measured Mo-to-S atomic ratio is around ~0.54, which is consistent with the stoichiometric ratio of MoS_2 (1:2). However, the measured Mo-to-C ratio is around ~0.55:1 which slightly differs from their corresponding precursor ratios 0.5:1. This phenomenon could be attributed to the partially oxidized MoS_2 to MoO_x that consistent to later XPS investigation.

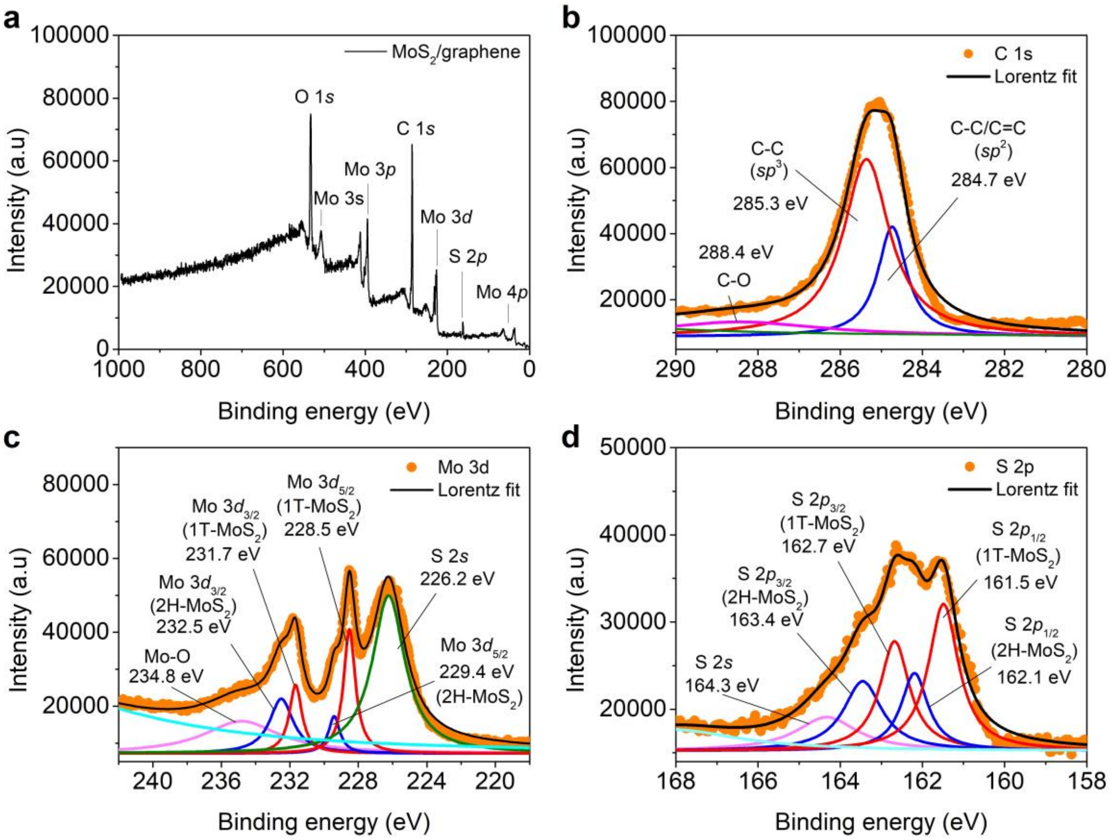

Figure 4. XPS spectra of MoS_2/graphene sample. (a) Full-scan spectrum (0–1000 eV), high-resolution core-level spectra of (b) C 1*s*, (c) Mo 3*d*, (d) S 2*p*.

To further confirm the chemical composition and chemical states of elements in MoS_2/graphene composite, the XPS measurements were performed. As shown in Figure 4(a), the survey wide range spectrum of MoS_2/graphene composite recorded from 0 to 1000 eV reveals the presence of Mo, S and C elements in the sample. Figure 4(b) shows the high resolution scan XPS with Lorentz peak-fitting result of C 1*s* region. One can see three resolved peaks of sp^2-hydridized C−C/C=C at ~284.7 eV, sp^3 (amorphous carbon) C−C at ~285.3 eV and oxygenated functional groups (C−O) at ~288.4 eV. The absence of the C(O)−O and C=O peaks indicates that the GO sheets have been almost reduced to graphene. From the high resolution scan spectrum of the Mo 3*d* region in Figure 4(c), two major peaks at ~228.5 and ~231.7 eV are observed which is assigned to the Mo^{+4} $3d_{5/2}$ and Mo^{+4} $3d_{3/2}$ in 2*H*-MoS_2, confirming the dominance of Mo(IV) in MoS_2/graphene sample. Besides the Mo(IV) $3d_{5/2}$ signal, a peak appears at ~226.2 eV which could be from the S 2*s* orbital. Also, a two shoulder located at ~229.4 and 232.5 eV corresponds to Mo^{+4} $3d_{5/2}$ and Mo^{+4} $3d_{3/2}$ in 1*T*-MoS_2 phase [36, 37]. Also a low broad peak at ~ 234.8 eV indicates molybdenum Mo(VI) in an octahedral configuration, which is typically observed in partially oxidized MoS_2 to MoO_3 phase. Another peak at higher binding energy of ~235.9 eV relates to the Mo ions in the +6 oxidation state, which may be due to the inadequate reduction of MoO_4^{2-} species during the hydrothermal synthesis. From the higher resolution XPS spectrum of the S 2*s* in Figure 4(d), the main doublet located at binding energies of ~161.5 and ~162.7 eV corresponds to the S $2p_{1/2}$ and S $2p_{3/2}$ of pristine MoS_2, respectively, which is consistent with previous reports [38, 39]. Based on the XPS investigation, the formation of MoS_2/graphene nanocomposite and the extent of reduction of GO to graphene can be successfully explained.

4. CONCLUSION

In summary, MoS_2/graphene nanocomposite has been successfully synthesized by simple, scalable and cost-effective hydrothermal technique. The results of FESEM, TEM, HRTEM, XRD, Raman spectroscopy, XPS and EDX showed that the 2H-MoS_2 nanosheets with a thickness less than of eight layers and lateral size of several hundred nanometers attached on the graphene surfaces, resulting in the formation of 3D architecture of MoS_2/graphene nanocomposite. Our approach is promising for a scalable, inexpensive, and accurate strategy to fabricate state-of-the-art materials with a certain structure for various practical applications such as electrode material for batteries or supercapacitor.

Acknowledgements. This work was supported by Vietnam National University Ho Chi Minh City (VNU-HCM) under grant number C2018-20-16.

REFERENCES

1. Wang Q. H., Kalantar-Zadeh K., Kis A., Coleman J. N. and Strano M. S. – Electronics and optoelectronics of two-dimensional transition metal dichalcogenides, Nat. Nanotechnol
2. **7** (2012) 699–712.
3. Novoselov K. S., Jiang D., Schedin F., Booth T. J., Khotkevich V. V., Morozov S. V. and Geim A. K. – Two-dimensional atomic crystals, Proc. Natl. Acad. Sci. U.S.A. **102** (2005) 10451–10453.
4. Geim A. K. – Nobel Lecture: Random walk to graphene, Rev. Mod. Phys. **83** (3) (2011) 851–862.
5. Novoselov K. S., Geim A. K., Morozov S. V., Jiang D., Zhang Y., Dubonos S. V., Grigorieva I. V. and Firsov A. A. – Electric field effect in atomically thin carbon films, Science **306** (2004) 666–669.
6. Castro Neto A. H., Guinea F., Peres N. M. R., Novoselov K. S. and Geim A. K. – The electronic properties of graphene, Rev. Mod. Phys. **81** (2009) 109–162.
7. Abergel D. S. L., Apalkov V., Berashevich J., Ziegler K., Chakraborty T. – Properties of graphene: a theoretical perspective, Advances in Physics **59** (2010) 261–482.
8. Radisavljevic B., Radenovic A., Brivio J., Giacometti V., Kis A. – Single-layer MoS_2 transistors, Nat. Nanotechnol. **6** (2011) 147–150.

9. Mak K. F., Lee C., Hone J., Shan J. and Heinz T. F. – Atomically thin MoS_2: A new direct-gap semiconductor, Phys. Rev. Lett. **105** (2010) 136805–136808.
10. Kuc A. – Low-dimensional transition-metal dichalcogenides, in SPR Chemical modelling: volume 11, M. Springborg, and J. Joswig, ed. London, UK: The Royal Society of Chemistry (2015) 1–29.
11. Xiang Q., Yu J. and Jaroniec M. – Synergetic effect of MoS_2 and graphene as cocatalysts for enhanced photocatalytic H_2 production activity of TiO_2 nanoparticles, J. Am. Chem. Soc. **134** (2012) 6575–6578.
12. David L., Bhandavat R. and Singh G. – MoS_2/graphene composite paper for sodium-ion battery electrodes, ACS Nano **8** (2014) 1759–1770.
13. Perkins F. K., Friedman A. L., Cobas E., Campbell P. M., Jernigan G. G. and Jonker B. T. – Chemical vapor sensing with monolayer MoS_2, Nano Lett. **13** (2) (2013) 668–673.
14. Bernardi M., Palummo M. and Grossman J. C. – Extraordinary sunlight absorption and one nanometer thick photovoltaics using two-dimensional monolayer materials, Nano Lett. **13** (2013) 3664–3670.
15. Hu Y., Li X., Lushington A. P., Cai M. R., Geng D.-S., Banis M. N., Li R. and Sun X. A. – Fabrication of MoS_2-graphene nanocomposites by layer-by-layer manipulation for high-performance lithium ion battery anodes, ECS J. Solid State Sci. Technol. **2** (2013) M3034–M3039.
16. Coleman J. N., Lotya M., O'Neill A., Bergin S. D., King P. J., Khan U., Young K., Gaucher A., De S., Smith R. J., Shvets I. V., Arora S. K., Stanton G., Kim H. Y., Lee K., Kim G. T., Duesberg G. S., Hallam T., Boland J. J., Wang J. J., Donegan J. F., Grunlan J. C., Moriarty G., Shmeliov A., Nicholls R. J., Perkins J. M., Grieveson E. M., Theuwissen K., McComb D. W., Nellist P. D. and Nicolosi V. – Two-dimensional nanosheets produced by liquid exfoliation of layered materials, Science **331** (2011) 568–571.
17. Ma L., Huang G., Chen W., Wang Z., Ye J., Haiyang L., Chen D. N. S. and Lee J. Y. – Cationic surfactant-assisted hydrothermal synthesis of few-layer molybdenum disulfide/graphene composites: Microstructure and electrochemical lithium storage, J. Power Sources **264** (2014) 262–271.
18. Hu H., Zhao Z., Wan W., Gogotsi Y. and Qiu J. – Ultralight and highly compressible graphene aerogels, Adv. Mater. **25** (2013) 2219–2223.
19. Guo J., Chen X., Jin S., Zhang M. and Liang C. – Synthesis of graphene-like MoS_2 nanowall/graphene nanosheet hybrid materials with high lithium storage performance, Catalysis Today **246** (2015) 165–171.
20. Song H., Tang A., Xu G., Liu L., Yin M., and Pan Y. – One-step Convenient Hydrothermal Synthesis of MoS_2/RGO as a High-performance Anode for Sodium-ion Batteries, Int. J. Electrochem. Sci. **13** (2018) 4720–4730.
21. Bing Z., Wang Z., Gao Y., Chen L., Lu M., Jiao Z., Jianga Y., Ding Y.-Zh. and Cheng L. – Hydrothermal synthesis of layer-controlled MoS_2/graphene composite aerogels for lithium-ion battery anode materials, Appl. Surf. Sci. **390** (2016) 209–215.
22. Thangappan R., Kalaiselvam S., Elayaperumal A., Jayavel R., Rivanandhan M., Karthikeyane R. and Hayakawa Y. – Graphene decorated with MoS_2 nanosheets: Synergetic Energy Storage composite electrode for Supercapacitor Applications, Dalton Trans. **45** (2016) 2637–2646.

23. Zhou W., Zhou K., Hou D., Liu X., Li G., Sang Y., Liu H., Li L. and Chen S. – Three-Dimensional Hierarchical Frameworks Based on MoS_2 Nanosheets Self-Assembled on Graphene Oxide for Efficient Electrocatalytic Hydrogen Evolution, ACS Appl. Mater. Interfaces **6** (2104) 21534–21540.
24. Hu L., Ren Y., Yang H. and Xu Q. – Fabrication of 3D Hierarchical MoS_2/Polyaniline and MoS_2/C Architectures for Lithium-Ion Battery Applications, ACS Appl. Mater. Interfaces **6** (2014) 14644–14652.
25. Zhang F., Tang Y., Liu H., Ji H., Jiang C., Zhang J., Zhang X. and Lee C.-S. – Uniform Incorporation of Flocculent Molybdenum Disulfide Nanostructure into Three-Dimensional Porous Graphene as an Anode for High-Performance Lithium Ion Batteries and Hybrid Supercapacitors, ACS Appl. Mater. Interfaces **8** (2016) 4691–4699.
26. Chang K. and Chen W. – In situ synthesis of MoS_2/graphene nanosheets composites with extraordinarily high electrochemical performance for lithium ion batteries, Chem. Commun. **47** (2011) 4252–4254.
27. Zheng X., Xu J., Yan K., Wang H., Wang Z. and Yang S. – Space-Confined Growth of MoS_2 Nanosheets within Graphite: The Layered Hybrid of MoS_2 and Graphene as an Active Catalyst for Hydrogen Evolution Reaction, Chemistry of Materials **26** (2014) 2344–2353.
28. Huang G., Chen T., Chen W., Wang Z., Chang K., Ma L., Huang F., Chen D. and Lee J. Y. – Graphene-like MoS_2/graphene composites: Cationic surfactant-assisted hydrothermal synthesis and electrochemical reversible storage of lithium, Small **9** (2013) 3693–3703.
29. Khai T. V., Na H. G., Kwak D. S., Kwon Y. J., Ham H., Shim K. B. and Kim H. W. – Influence of N-doping on the structural and photoluminescence properties of graphene oxide films, Carbon **50** (2012) 3799–3806.
30. Khai T. V., Na H. G., Kwak D. S., Kwon Y. J., Ham H., Shim K. B. and Kim H. W. – Significant enhancement of blue emission and electrical conductivity of N-doped graphene, J. Mater. Chem. **22** (2012) 17992–18003.
31. Chang K., Mei Z., Wang T., Kang Q., Ouyang S. and Ye J. – MoS_2/graphene cocatalyst for efficient photocatalytic H_2 evolution under visible light irradiation, ACS Nano **8** (2014) 7078–7087.
32. Cui Y. R., He J. S., Li X. M., Zhao J. X., Chen A. L. and Yang J. – Preparation and characterization of MoS_2 microsphere by hydrothermal method, Adv. Mater. Res. **631** (2013) 306–309.
33. Geng X., Sun W., Wu W., Chen B., Al-Hilo A., Benamara M., Zhu H., Watanabe F., Cui J. and Chen T. P. – Pure and stable metallic phase molybdenum disulfide nanosheets for hydrogen evolution reaction, Nat. Commun. **7** (2016) 10672–10677.
34. Kudin K. N., Ozbas B., Schniepp H. C., Prud'homme R. K., Aksay I. A. and Car R. – Raman spectra of graphite oxide and functionalized graphene sheets, Nano Lett. **8** (2008) 36–41.
35. Ferrari A. C., Meyer J. C., Scardaci V., Casiraghi C., Lazzeri M., Mauri F., Piscanec S., Jiang D., Novoselov K. S., Roth S. and Geim A. K. – Raman spectrum of graphene and graphene layers, Phys. Rev. Lett. **97** (2006) 187401(1)–187401(4).

36. Bosch-Navarro C., Coronado E., Martí-Gastaldo C., Sánchez-Royo J. F. and Gómez M. – Influence of the pH on the synthesis of reduced graphene oxide under hydrothermal conditions, Nanoscale **4** (2012) 3977–3982.
37. Kibsgaard J., Chen Z., Reinecke B. N. and Jaramillo T. F. – Engineering the surface structure of MoS_2 to preferentially expose active edge sites for electrocatalysis, Nat. Mat. **11** (2012) 963–969.
38. Guo Y., Sun D., Ouyang B., Raja A., Song J., Heinz T. F. and Brus L. E. – Probing the Dynamics of the Metallic-to-Semiconducting Structural Phase Transformation in MoS_2 Crystals, Nano Lett. **15** (2015) 5081−5088.
39. Fan H., Wu R., Liu H., Yang X., Sun Y. and Chen C. – Synthesis of metal-phase-assisted 1T@2H-MoS_2 nanosheet-coated black TiO_2 spheres with visible light photocatalytic activities, J. Mat. Sci. **53** 10302–10312.
40. Fan X., Xu P., Zhou D., Sun Y., Li Y. C., Nguyen M. A. T., Terrones M. and Mallouk T. E. – Fast and Efficient Preparation of Exfoliated 2H-MoS_2 Nanosheets by Sonication-Assisted Lithium Intercalation and Infrared Laser-Induced 1T to 2H Phase Reversion, Nano Lett. **15** (2015) 5956–5960.